J. Electrochem. Sci. Eng. **15(3)** (2025) 2607; http://dx.doi.org/10.5599/jese.2607

Open Access : : ISSN 1847-9286
https://pub.iapchem.org/ojs/index.php/JESE

Original scientific paper

Improving the corrosion behaviour of Zn-Ni alloy coatings on 316 SS from chloride-sulfate bath by addition of triethanolamine or sucrose

Mothana Ghazi Kadhim AlFalah[1,✉], Ali H. Abbar[2] and Fatma Kandemirli[3]

[1]*Materials of Engineering Department, College of Engineering, University of Al-Qadisiyah, Al-Diwaniyah, Iraq*
[2]*Department of Biochemical Engineering, Al-Khwarizmi College of Engineering, University of Baghdad, Baghdad, Iraq*
[3]*Department of Biomedical Engineering, Faculty of Engineering and Architecture, Kastamonu University, Turkey*

**Corresponding Author: E-mail: ✉mothana.kadhim@qu.edu.iq*

Received: December 21, 2024; Accepted: March 31, 2025; Published: April 2, 2025

Abstract

Corrosion of Zn-Ni alloy coatings on stainless steel 316 SS in a chloride-sulfate bath with the addition of either triethanolamine or sucrose was examined. A constant cathode potential was used to deposit zinc-nickel alloys, while cyclic voltammetry and potentio-dynamic polarization were used to measure corrosion. In addition, scanning electron microscopy was utilized to analyse Zn-Ni alloy coating surface layers formed without and with additives. The outcomes discovered that the corrosion resistance of Zn-Ni alloy coatings in 3.5 % NaCl solution was highly influenced by adding triethanolamine or sucrose. Decreasing the Zn:Ni molar ratio led to an increase in corrosion resistance. All Zn-Ni alloy coatings were superior to pure Zn coating in their corrosion behaviour. The best result was found for potentiostatic electrodeposition of Zn-Ni alloy at the cathodic potential of -1.3 V vs. Ag/AgCl for 20 minutes in the presence of 0.335 M triethanolamine from a solution containing 0.02 M $ZnCl_2$, 0.1 M $NiSO_4$, 0.4 M H_3BO_4 and 1 M Na_2SO_4. For this Zn-Ni coating, a low corrosion rate of 0.00795 mm year^{-1} was observed at E_{corr} = -0.5 V vs. Ag/AgCl and i_{corr}= 0.535 µA cm^{-2}. Scanning electron microscopy confirmed that this alloy has a granular structure with no cracks and a less porous structure. The new Zn-Ni alloy is superior in its properties in terms of corrosion resistance compared with those obtained in previous studies.

Keywords

Metal alloy coatings; electrodeposition; bath composition; organic additives; corrosion resistance

Introduction

Numerous authors examined the corrosion properties of iron alloys. Some of these alloys are characterized by their excellent resistance to corrosion in various corrosive environments, but others are subject to localized corrosion when chloride ions are present [1]. Cooling systems that used seawater as a coolant in their operations as well as equipment used in the desalination industry, suffer solely from degradation due to the presence of extremely violent Cl^- ions, which demolished oxide films that were secured against corrosion for metals and alloys. Therefore, when used in corrosive environments containing chloride ions, most carbon steel alloys have to be coated [2].

Zinc alloy deposits, particularly with iron group metals such as Fe, Ni, and Co, have demonstrated better mechanical, physical and electrochemical properties than pure zinc [3,4]. Consequently, the interest in such alloys was recently assessed due to their superior corrosion resistance [5]. Zn-Ni alloys are the most widely used to provide sacrificial protection to steel and its alloys. They were used to replace expensive and harmful Cd coatings in anti-corrosion applications such as electronics and automotive, aerospace and electricity industries [6].

Austenitic stainless steel is a novel material becoming increasingly popular as a bone implant. It is believed that bone implants made of 316L stainless steel may temporarily support diseased or healing tissues. Austenitic stainless steel has been regarded as exceptional due to its appropriate mechanical properties, low casting, and decent corrosion resistance. The existence of a thin protective chromium-enriched oxide coating is linked to 316 SS resistance to corrosion in an aqueous environment. 316 SS has some disadvantages, such as pitting corrosion that releases metal ions, including nickel, chromium, and molybdenum, reducing material biocompatibility and long-term performance [7].

The application of a Zn-Ni coating on a stainless steel substrate significantly improves corrosion resistance in highly harsh settings, including marine, supercritical water containing NaOH, chloride molten salts in solar energy storage and chemical industries [8,9]. Furthermore, 316SS generally has a smoother and more uniform surface than other iron alloys, such as mild steel, which may exhibit surface imperfections and impurities. This homogeneity may enhance adhesion and provide more constant Zn-Ni coating deposition, resulting in a superior finish [10,11].

Electrodeposition of zinc-nickel composite was classified as unpredictable deposition [12]. There is a higher ratio of zinc in coatings despite nickel being nobler than zinc. Zn-Ni alloy electrodeposition in an electrolyte environment, however, is not always problematic, as certain experimental circumstances allow electrodeposition of nickel-rich alloys [13]. Zinc-nickel alloy corrosion properties are influenced by its composition, where increasing Zn quantities shift corrosion potential to more negative values due to the sacrificial character of Zn while increasing Ni quantities shift the corrosion potential to less negative values due to the barrier character of Ni [14]. However, raising the nickel content to higher amounts does not often produce improved outcomes, with the coating being a strong impediment because once cracked or damaged, the substrate is no longer covered [15].

Many studies have shown that nickel content is an important parameter affecting the corrosion resistance of deposits [14,16]. The corrosion protection of Zn-Ni alloys depends on the composition of the phase in the alloy, which is affected by various parameters such as the applied current density, the Zn:Ni molar ratio in the bath, the temperature and the pH of solution [17,18].

Five phases for zinc-nickel alloys have been recognized: η-(1 % Ni), α and β-(30 % Ni) identified the phases rich in nickel, and δ-(Ni_3Zn_{22}) and γ-(Ni_5Zn_{21}) as the phases rich in zinc [19,20]. The γ phase composite shows the best corrosion resistance, with nickel content between 8 and 15 %, and

(cc) BY

therefore, more examinations have been done widely on this phase [19]. In acidic baths γ and δ phases were observed [21].

Two types of electrolytic baths, *i.e.* the acid bath and the alkaline bath, can be used to deposit zinc-nickel alloy. The acid bath consists of a mixture of zinc and nickel salts (sulfates, chlorides, or a mixture of them), buffers and optional brighteners [21,22]. In the alkaline type, the electrolyte involves NaOH and additives to keep the metal species in solution [23-25]. Acid bath allows a higher deposition rate and cathodic efficiency; therefore, it was used extensively. Moreover, the acid bath ensures a low-cost deposition process compared to the alkaline plating bath because no complexing agents are required [26].

The use of organic additives in electrodeposition baths of Zn alloys is very important due to their internal effects on the progress and structure of subsequent deposits. The addition of these compounds has been reported to influence mechanical, physical and electrochemical properties of alloys, such as grain size, internal stress, brightness, pitting, and even chemical structure [23-25,27,28]. Rare research on the use of triethanolamine as a chemical addition for Zn-Ni alloy preparation has also been published. Triethanolamine was used with moderately low antimicrobial and plant-development animating exercises. Triethanolamine is, however, a well-known compound attributable to specialized applications as a healing agent for epoxy and elastic polymers, glues and antistatic agents, and as a corrosion inhibitor for metals [29]. For example, Ravindran and Muralidharan [28] studied the effect of triethanolamine on zinc-nickel alloy plating from the bath with sulfamate, showing that triethanolamine increases current plating process efficiency and provides a homogenous, smooth grayshell deposit with smaller crystallites on stainless steel. Triethanolamine was also used in the electrodeposition of Zn-Ni alloy from zincate solutions as a complexing agent for Ni^{2+} ions [23,24].

Hammami *et al.,* [27] analysed the performance of diethanolamine (DEA) and triethanolamine (TEA) on zinc-nickel alloy coating from acid sulfate solution on steel substrates. They found that the Zn-Ni alloy electrodeposited in the mM range for TEA concentration showed better corrosion resistance than the unaltered Zn-Ni combination electrodeposited under comparable conditions. However, no study has been published on the impact of triethanolamine on the corrosion actions of Zn-Ni alloys in sodium chloride solution when these alloys are prepared from a chloride-sulfate solution by electrodeposition on a stainless steel substrate.

Sucrose has been used as an ingredient in several zinc electroplating baths to enhance deposit characterization [30,31]. However, no research has been performed on utilizing of sucrose as an additive in the electrodeposition of Zn-Ni alloy.

The aim of this research is to examine the electrodeposition of zinc-nickel alloys from chloride-sulfate baths containing triethanolamine or sucrose as additives by applying constant cathode potential while studying their effect on the corrosion resistance of Zn-Ni coatings. The investigation was accomplished using cyclic voltammetry (CV), potentiostatic electrodeposition, and potentiodynamic polarization techniques. In addition, scanning electron microscopy (SEM) and energy dispersive X-ray spectroscopy (EDX) were used to investigate the topography of Zn-Ni coatings electrodeposited under the best conditions.

Experimental

Cyclic voltammetry experiments were performed under stagnant conditions using three-electrode cell with size 100 cm^3 at a potential range from +0.5 to -1.6 V *vs*. Ag/AgCl, with a scan rate of 2 mV s^{-1}. A stainless steel plate (316L) was employed as a working electrode with a surface area of 0.785 cm^2. It has a chemical composition of 16.70 wt.% Cr, 12.20 wt.% Ni, 2.10 wt.% Mo, 1.32 wt.% Mn, 0.56 wt.%

Si, 0.03 wt.% P, 0.022 wt.% C, 0.012 wt.% S, 0.26 wt.% Cu, (Fe balance). Platinum wire was used as a counter electrode while Ag/AgCl electrode (E^o= 0.208V *vs*. SHE) has been used as a reference electrode. All potentials were recorded with respect to the Ag/AgCl electrode.

The electrodeposition solution included $ZnCl_2$ and $NiSO_4{\cdot}7H_2O$ at different concentrations as sources of Zn and Ni ions, 1 M Na_2SO_4 as a supporting electrolyte, 0.4 M H_3BO_4 as a buffer agent, and either triethanoleamine, or sucrose as additives at concentrations of 0.335 and 0.015 M, respectively. The value chosen for the concentration of triethanolamine was based on observations of Nakano *et al*. [23] that this concentration offers greater complexity to the nickel ions and enhances the structural and morphological properties of the Zn-Ni alloy coatings to be more fine and compact structures. Fructose, lactose, sucrose and D-glucose are typically used in zinc plating at concentrations of 4 to 6 g L^{-1} [30]. Therefore, the value of sucrose concentration was taken between these values in the present research. By utilizing H_2SO_4 and sodium hydroxide, the pH of the solutions was held at 3. All chemicals used in the experiments were of analytical grades (Merck). Doubly distilled water was used to prepare all solutions.

Zn-Ni alloys were potentiostatically deposited from a sulfate-chloride bath on stainless steel. Before actual electrodeposition, each specimen was carefully polished with emery paper, starting from 600 to 1200 grades, then degreased in an alkaline solution consisting of sodium carbonate and sodium hydroxide, and finally rinsed with distilled water. All tests were conducted using computerized potentiostat (type DY2322, USA) at ambient temperature.

Corrosion performances of Zn, Ni and Zn-Ni alloy coatings were investigated using a potentiodynamic polarization (PDP) technique at ±500 mV with respect to open circuit potential at a scan rate of 1 mV s^{-1} in 3.5 % NaCl solution maintained at 25 °C. The same electrolytic cell used in cyclic voltammetry experiments was used in the corrosion experiments with one exception that the stainless steel substrate was coated previously with either Zn, Ni, or Zn-Ni coatings for 20 min at constant values of cathodic potential based on the cyclic voltammetry results. All experiments were repeated with satisfactory reproductive measurements and a deviation of less than 5 %. A scanning electron microscope (FEG 250 SEM (FEI-Quanta, Hillsboro, OR, USA) was used to investigate the topography of zinc-nickel alloy coatings formed with and without additives.

Results and discussion

Cyclic voltammetry

In order to consider the effect of additives, cyclic voltammetry for electrodeposition of Ni, Zn, and Zn-Ni alloys was carried out at 25°C on a stainless steel substrate. Figure 1 displays cyclic voltammograms for 316L stainless steel submerged in solutions comprising of pure zinc ion (0.1 M $ZnCl_2$), pure nickel ion (0.1 M $NiSO_4$) and a combination of them (0.1 M $ZnCl_2$ + 0.1 M $NiSO_4$), in 1M Na_2SO_4 as the supporting electrolyte.

As zinc is less noble than nickel, its deposition occurs at an electrode potential that is more negative than nickel electrodeposition. Electrodeposition of zinc starts at around -1.1 V, while co-deposition of Zn-Ni begins at around -1.2 V. It became obvious that the Zn-Ni deposition is initially moved significantly towards more negative potentials relative to pure Ni and pure Zn baths. Reverse scans show anodic peaks at -0.66 and -0.10 V, referring to the dissolution of zinc and nickel deposited from the baths of pure metals, while the dissolution of Zn-Ni alloy reveals two small peaks within the potential range (-0.8 to -0.4 V). It was found in a mixed solution that anodic dissolution potentials of zinc and nickel metals are moved, suggesting that when mixed, metals influence one another's

(cc) BY

deposition. The necessity of dissolving metal peaks relative to each other is expected to exist because most of the Zn-Ni alloys undertake anomalous deposition [15].

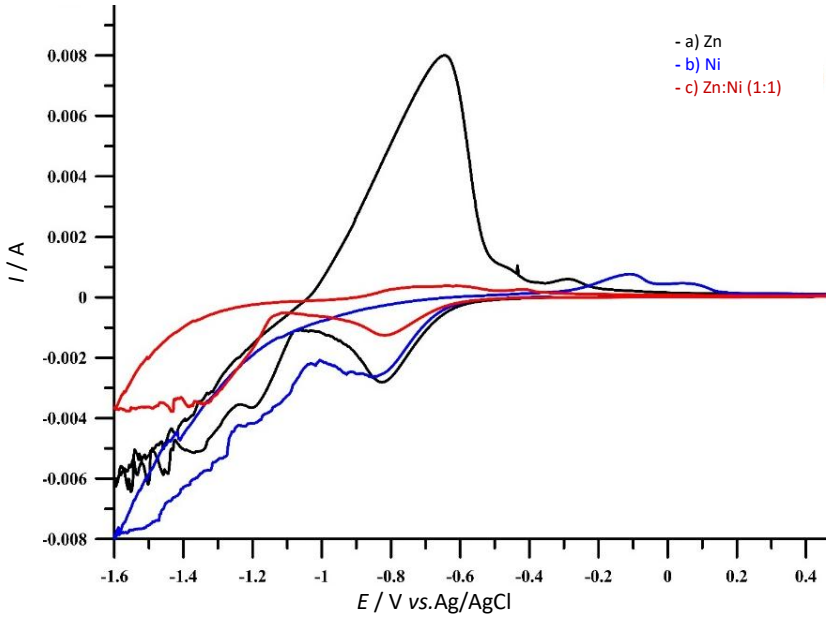

Figure 1. *Cyclic voltammograms (scan rate 2 mV s^{-1}) for 316L SS in: a) 0.1 M $ZnCl_2$; b) 0.1 M $NiSO_4$; c) 0.1 M $ZnCl_2$ + 0.1 M $NiSO_4$. Supporting electrolyte: 1M Na_2SO_4, pH 3*

Figures 2 to 4 show the influence of Zn:Ni molar ratio on the cyclic voltammograms of Zn-Ni alloys electrodepostion on a stainless steel substrate. All curves display two peaks of oxidation, but their position and height differ according to Zn:Ni molar ratio. The first peak of oxidation appears at around 0.85 V, and its height rises by raising the proportion of Zn:Ni molar ratio above one. At the same time, the second peak of oxidation appears at -0.4 V, and its height declines as the Zn:Ni molar ratio increases above one. When the molar ratio Zn:Ni is less than one, two peaks move to more positive potential. However, Zn:Ni (1:1) provides roughly the same height as the two oxidation peaks.

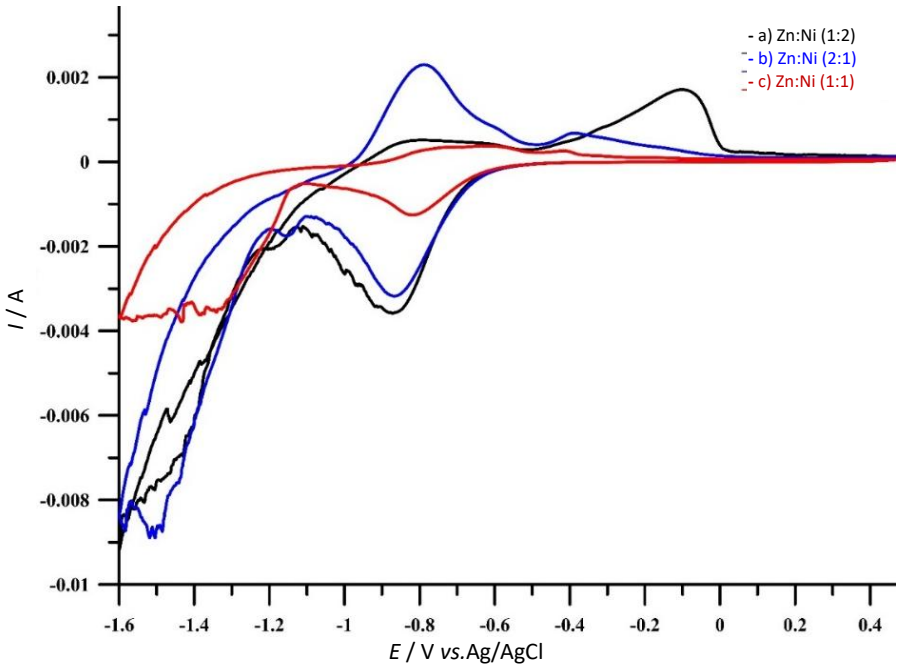

Figure 2*. Cyclic voltammograms (scan rate 2 mV s^{-1}) for 316L SS in: a) 0.05 M $ZnCl_2$+0.1 M $NiSO_4$; b) 0.1 M $ZnCl_2$+0.05 M $NiSO_4$, c) 0.1 M $ZnCl_2$+0.1 M $NiSO_4$. Supporting electrolyte: 1 M Na_2SO_4, pH 3*

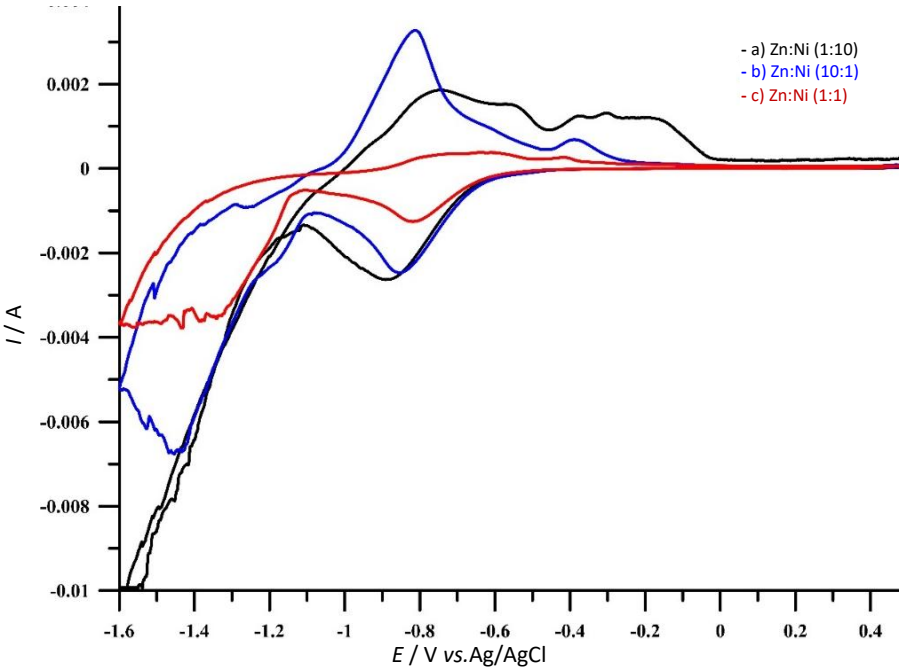

Figure 3. *Cyclic voltammograms (scan rate 2 mV s^{-1}) for 316L SS in: a) 0.02 M $ZnCl_2$+0.1 M $NiSO_4$; b) 0.1 M $ZnCl_2$+0.02 M $NiSO_4$; c) 0.1 M $ZnCl_2$+0.1 M $NiSO_4$. Supporting electrolyte: 1 M Na_2SO_4, pH 3*

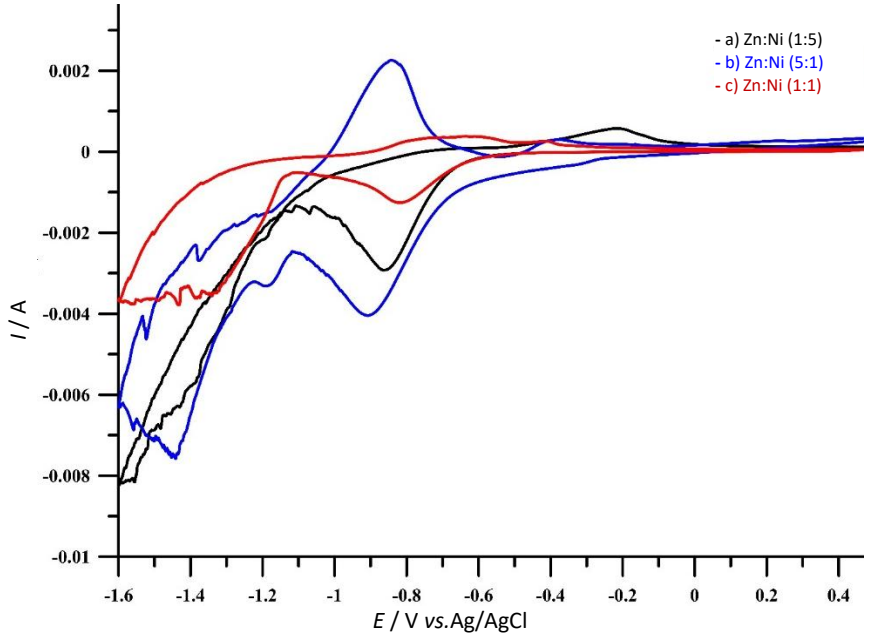

Figure 4. *Cyclic voltammograms (scan rate 2 mV s^{-1}) for 316L SS in: a) 0.0 1 M $ZnCl_2$+0.1 M $NiSO_4$; b) 0.1 M $ZnCl_2$+0.01 M $NiSO_4$; c) 0.1 M $ZnCl_2$+0.1 M $NiSO_4$. Supporting electrolyte: 1 M Na_2SO_4, pH 3*

CV tests were conducted to illustrate the effect of additives, as shown in Figure 5. Significant changes are found during the cathodic scan, especially for H_3BO_4 additions alone or in combination with triethanolamine or sucrose. With the addition of additives, the starting deposition potential is shifted from -0.52 to -0.65 V. However, the deposition potential of the Zn-Ni alloy was observed at around -1.2 V. During the anodic potential scan, three oxidation peaks were distinctly noted at -0.735, -0.527 and -0.432 V, respectively, when H_3BO_4 was used alone or in collaboration with sucrose. These three voltammetric peaks correspond to the formation of three phases, as proved by previous works [24,29,30]. The two anodic peaks at -0.735 and -0.527 V refer to zinc dissolution from δ-phase (Ni_3Zn_{22}) and γ-phase (Ni_5Zn_{21}), respectively, while the anodic peak at more noble potential (-0.432 V) refers to nickel dissolution from its phases.

(cc) BY

The condition was different when H_3BO_4 was used in combination with triethanolamine; two oxidation peaks were found at -0.6 and -0.37 V, respectively. Such peaks are moved to more positive potentials, suggesting an improvement in the Ni content [32]. The heights of oxidation peaks are often greater with than without additives, with a maximum being in the case of the addition of both H_3BO_4 and sucrose. An exception was characterized with respect to the addition of H_3BO_4 with triethanolamine where the peak heights are lower than with the addition of H_3BO_4 alone. The present results are in agreement with the suggestion provided by Gomez *et al.* and Trejo *et al*. [33,34] that the existence of several anodic alloy peaks can be due to the dissolution of numerous intermediate phases. Hammami *et al*. [27] found that the addition of triethanolamine impacts Zn-Ni co-deposition and changes the alloy structure. To ensure the formation of Zn-Ni co-deposits, a negative potential greater than -1.1 V should be applied. Thus, given the cyclic voltammetry curves, the cathodic potential of -1.3 V was selected for the deposition of Zn and Zn-Ni alloys.

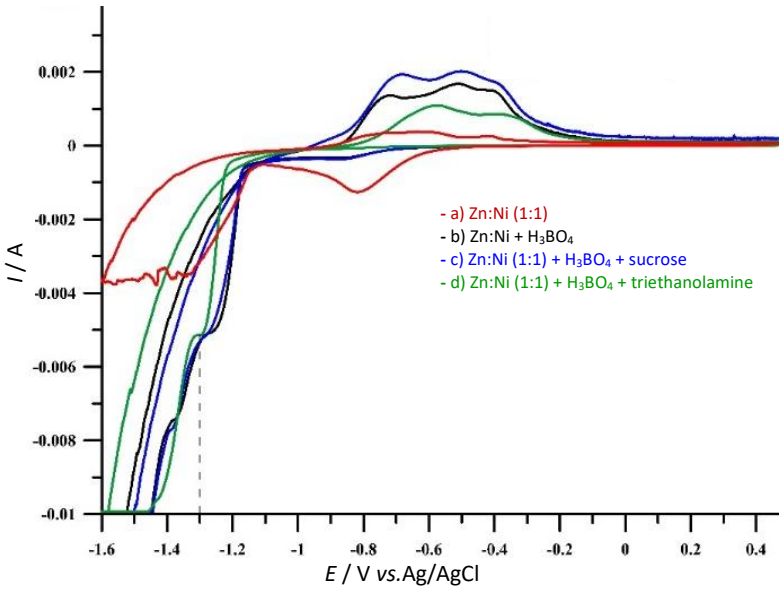

Figure 5. *Cyclic voltammograms (scan rate 2 mV s^{-1}) for 316L SS in 0.1 M $ZnCl_2$ + 0.1 M $NiSO_4$: a) without additives, and with b) 0.4 M H_3BO_4; c) 0.4 M H_3BO_4 +0.015 M sucrose; d) 0.4 M H_3BO_4 + + 0.335 M triethanolamine. Supporting electrolyte: 1 M Na_2SO_4, pH 3*

Corrosion studies

The potentiodynamic polarization (PDP) technique was used to test corrosion properties of zinc coatings on stainless steel and Zn-Ni coatings formed in the presence and absence of triethanolamine or sucrose in a 3.5 % NaCl corrosive environment. For comparison, stainless steel substrate was also examined. The corrosion potentials were calculated from the PDP curves, which show the behaviour of the deposits in a corrosive environment. Figure 6 displays the Tafel plots for stainless steel without coating and with zinc coating in 3.5 % NaCl solution. 316L SS has a corrosion potential of -0.4 V, while zinc has a corrosion potential of -1.049 V, which is more negative than for stainless steel in the same conditions. The value of corrosion potential of stainless steel in the present work is in agreement with previous studies [35,36]. With respect to zinc coating, previous works showed that the zinc layer's composition is complex but is generally thought to consist of ZnO in combination with a porous layer, which results in an increase in corrosion rate [37]. Hence, a high corrosion rate of zinc (2.387 mm $year^{-1}$ was determined using the software that follows potentiostat type DY2322, USA by applied Tafel extrapolation and Faraday's law) was observed in the present work.

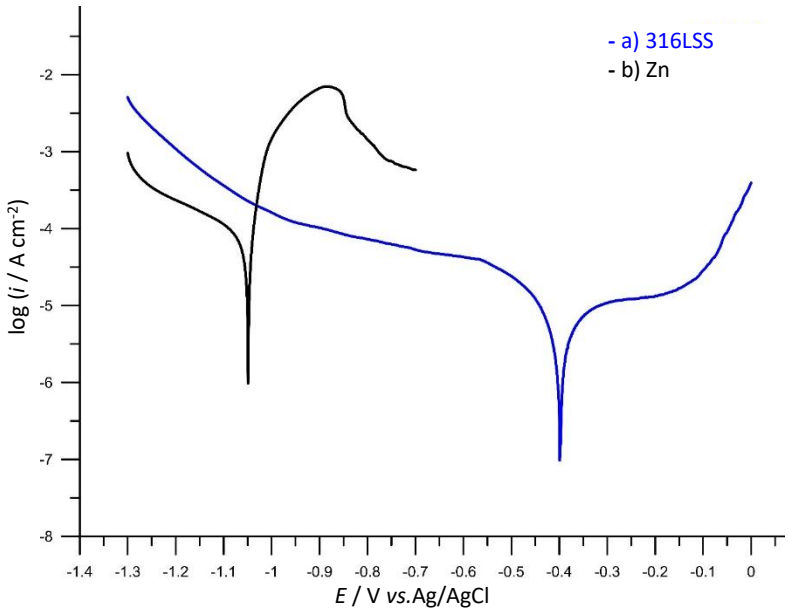

Figure 6. *Potentiodynamic polarization curves in logarithmic scale for: a) 316L SS; b) zinc deposit on 316L SS, in 3.5 wt.% NaCl solution*

Figure 7 shows the Tafel plots for Zn-Ni coatings on stainless steel in 3.5 % NaCl solution for Zn:Ni (1:1) and Zn:Ni (1:5) molar ratios without additives (triethanolamine or sucrose). It can be seen that the corrosion potentials of Zn-Ni coatings are more negative than those of stainless steel and less negative than those of zinc coatings. For Zn:Ni (1:1), E_{corr} = -0.801 V, while for Zn:Ni (1:5), E_{corr} = -0.666 V. This indicates that the Zn-Ni coatings offer sacrificial cathodic protection to stainless steel with higher corrosion resistance than zinc. In addition, it can be seen that the passive region area increased with the increase in the amount of nickel. It is well-known that increasing nickel concentration gives higher protection to the 316L SS substrate [16]. Thus, the enhancement achieved in the corrosion resistance of the alloy deposits may be attributed to the higher concentration of nickel.

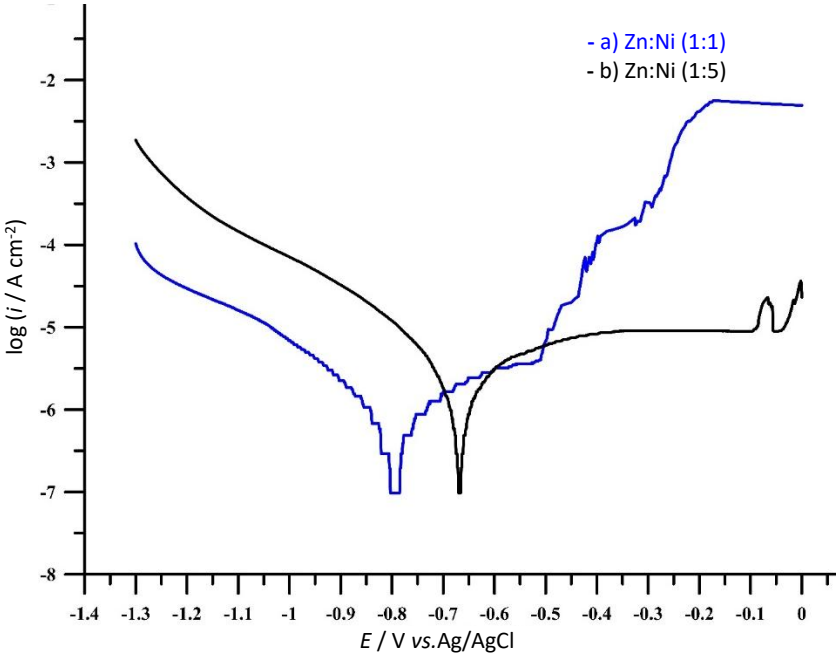

Figure 7. *Potentiodynamic polarization curves in logarithmic scale for Zn-Ni alloy deposits on 316L SS in 3.5 wt.% NaCl solution: a) Zn:Ni (1:1); b) Zn:Ni (1:5). Deposition conditions: 0.4 M H_3BO_4, 1 M Na_2SO_4, time = 20 min,* E *= -1.3 V* vs. *Ag/AgCl*

CC BY

When Zn-Ni alloy is corroded, zinc begins to dissolve, leaving a top layer enriched with nickel, which acts as a barrier to further attacks [32]. The present results are in agreement with the results of Ramanauskas *et al.* [37], in which the existence of 0.6 and 12 wt.% Ni in the matrix of zinc electrodeposits gives an improvement in the corrosion resistance of coatings in aerated chloride solutions.

Figure 8 shows the Tafel plots for Zn-Ni coatings on stainless steel in 3.5% NaCl solution for Zn:Ni (1:1) and Zn:Ni (1:5) molar ratios, with the addition of 0.335 M triethanolamine. The findings demonstrate major improvements in corrosion behaviour, where the addition of triethanolamine, in comparison with Zn-Ni coatings without triethanolamine, contributes to less negative corrosion potential. For Zn:Ni (1:1), the corrosion potential in the existence of triethanolamine was -0.439 V, while in the absence of triethanolamine, it was -0.801 V. On the other hand, it was found that the corrosion potential for Zn:Ni (1:5) with the addition of triethanolamine is -0.5 V. This behaviour may be due to the interaction of Zn and Ni ions with triethanolamine, leading to the consistency of compounds in which monodentate, bidentate, tridentate, or tetradentate binding modes could be demonstrated [38]. In addition, triethanolamine ligands are also ready to cooperate as crossings between two metal cations over ligands [39]. The addition of triethanolamine thus improves the protection against corrosion for stainless steel.

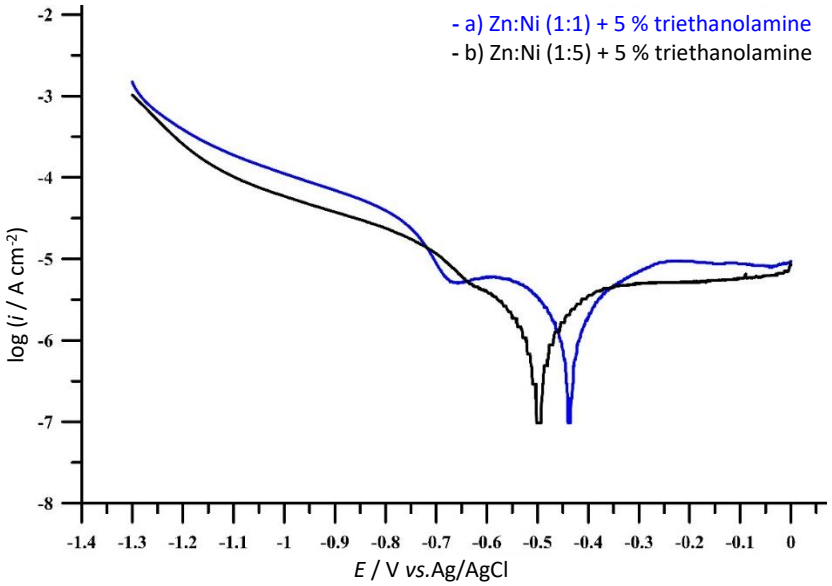

Figure 8. *Potentiodynamic polarization curves in logarithmic scale for Zn-Ni alloy deposits on 316L SS in 3.5 wt.% NaCl solution. Deposition conditions: a) Zn:Ni (1:1)+0.335 M triethanolamine; b) Zn:Ni (1:5) + 0.335 M triethanolamine, in 0.4 M H_3BO_4, 1 M Na_2SO_4; time = 20 min;* E= *-1.3 V* vs. *Ag/AgCl*

Figure 9 shows the Tafel plot for Zn-Ni coating on stainless steel in 3.5 % NaCl solution for Zn:Ni (1:1) with the addition of 0.015 M sucrose. It can be seen that the addition of sucrose gives the same response as triethanolamine, with a slightly higher corrosion rate than in the presence of triethanolamine. Its corrosion potential was -0.566 V and less negative than Zn-Ni coatings from a solution free of sucrose. Hence, the addition of sucrose also results in better corrosion protection for stainless steel.

As a complete tool for investigating the process of corrosion on the surface of the metal, the Tafel method also provides other corrosions parameters besides the corrosion potential (E_{corr}), such as corrosion current density (i_{corr}), polarization resistance (R_p) of the sample under study, and the rate of corrosion expressed as iron thickness corroded per year.

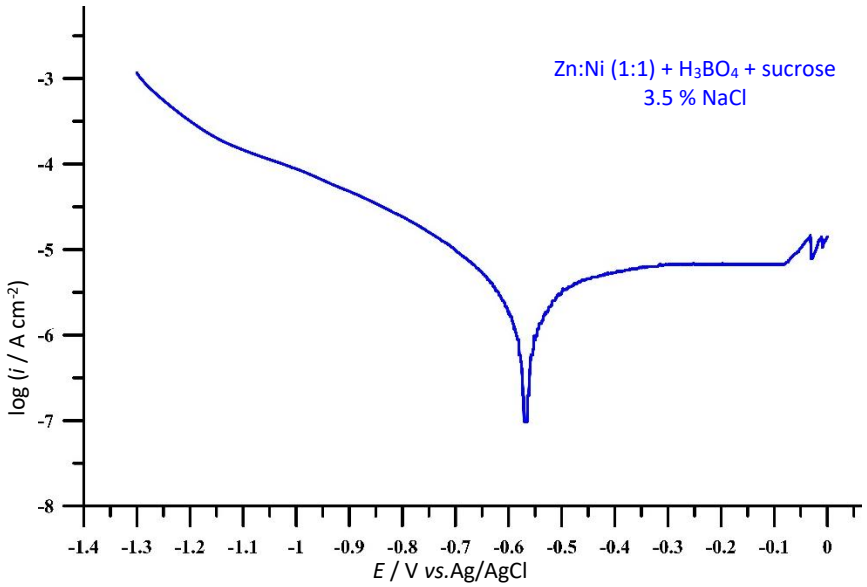

***Figure 9**. Potentiodynamic polarization curve in logarithmic scale for Zn-Ni alloy deposited on 316L SS in 3.5 wt.% NaCl solution. Deposition conditions Zn:Ni (1:1), 0.4 M H_3BO_4, 0.015 M sucrose, Na_2SO_4, time=20 min,* E *= -1.3 V* vs. *Ag/AgCl*

Table 1 displays the values of E_{corr} *vs*. Ag/AgCl), i_{corr} , corrosion rate and R_p , all values have been extracted from software following potentiostat by applied Tafel extrapolation and Faraday's law for pure zinc, and Zn-Ni alloys coatings under the study [40].

***Table 1.** Corrosion parameters obtained from Tafel polarization for 316SS, zinc and Zn-Ni alloys in 3.5 wt.% NaCl solution*

Metal or alloy	E_{corr} / V *vs*. Ag/AgCl	i_{corr} / μA cm^{-2}	Corrosion rate, mm year^{-1}	R_P / Ω cm^2
316SS	-0.398	3.89	0.022	5147
Zn	-1.049	124	2.387	162.1
Zn:Ni (1:1) + 0.4 M H_3BO_4	-0.801	0.986	0.01466	20442
Zn:Ni (1:5) + 0.4 M H_3BO_4	-0.666	0.64	0.0096	29555
Zn:Ni (1:1) + 0.4 M H_3BO_4 + + 0.335 M triethanolamine	-0.439	1.116	0.0165	18079
Zn:Ni (1:5) + 0.4 M H_3BO_4 + + 0.335 M triethanolamine	-0.5	0.535	0.00795	37680
Zn:Ni (1:1) + 0.4 M H_3BO_4 + + 0.015 M sucrose	-0.566	1.003	0.0149	20112

It can be seen that the potential corrosion shifted more negatively with the presence of the coating layer. This behaviour suggests that the deposition of coating molecules creates a protective layer on the metal surface, thereby reducing the number of active sites on the 316 SS surface. Furthermore, the corrosion rates were remarkably slowed down from 0.022 mm year^{-1} without coating (316L SS) to 0.0096 and 0.00795 mm year^{-1} with coatings Zn:Ni (1:5) + 0.4 M H_3BO_4 and Zn:Ni (1:5) + 0.4 M H_3BO_4 + 0.335 M triethanolamine, respectively. In other words, coatings Zn:Ni (1:5) + + 0.4 M H_3BO_4 and Zn:Ni (1:5) + 0.4 M H_3BO_4 + 0.335 M triethanolamine have been announced as good protection for stainless steel 316 due to the improvement of deposition layer on the 316 SS surface, thereby blocking violent ions from adhering to the metal's surface [41,42].

It seems that when using Zn-Ni coatings as a protection against stainless steel, there is a drastic decrease in the corrosion current density compared with pure zinc coverings. The corrosion current density of Zn-Ni coatings at Zn: Ni (1:5) with the addition of triethanolamine is more than two hundred times lower than obtained for zinc coating. It is clear that Zn-Ni coatings are characterized

(cc) BY

by higher values of polarization resistance. This is in accordance with the results of Wykpis *et al*. [22]. Table 1 reveals that Zn-Ni coating with Zn: Ni (1:5) with the addition of triethanolamine gives the best result as a protective coating of 316LSS.

Table 2 presents a comparison of corrosion potential and current density values obtained in the present work with some previous works. It can be seen that the results of the present work show better corrosion resistance than previous works due to the effect of triethanolamine addition. The corrosion potential is more positive than that obtained in the work of Faid *et al.* [32], with a drastic decrease in corrosion current density. However, the work of Wykpis *et al.* [22] showed a slightly lower corrosion current density due to the large molar ratio of Ni.

Table 2. *Comparison with previous studies related to preparation of Zn-Ni alloy and their corrosion behaviour*

Substrate	Bath	E_{corr} / V	i_{corr} / μA cm^{-2}	Ref.
AISI 301L	325 g L^{-1} $ZnSO_4$, 200 g L^{-1} $NiCl_2$, 40 ml L^{-1} glacialacetic acid, 0.1 g L^{-1} sodium lauryl sulphate	-1.143 V *vs.* SCE in 3.5 % NaCl	50	[35]
Austenitic steel (OH18N9)	160 g L^{-1} $NiSO_4{\times}7H_2O$, 24 g L^{-1} $NiCl_2{\times}6H_2O$, 14 g L^{-1} $ZnCl_2$, 40 g L^{-1} H_3BO_4, 30 g L^{-1} $MgSO_4$	-0.699 V *vs.* SCE In 5% NaCl	0.27	[22]
Steel STUB100CR6	57.5 g L^{-1} $ZnSO_4{\times}7H_2O$, 52.5 g L^{-1} $NiSO_4{\times}6H_2O$, 9.3 g L^{-1} H_3BO_4, 56.8 g L^{-1} Na_2SO_4:	-0.995 V *vs.* SCE in 3 % NaCl	-	[27]
Zn-Ni alloy (10 % Ni)	-	-1.032 V *vs.* SCE in 3.5 % NaCl	7.3	[16]
AISI 301L	0.2 M $ZnSO_4{\times}7H_2O$, 0.2 M $NiSO_4{\times}6H_2O$, 0.4 M H_3BO_4, 1 M Na_2SO_4	-1.122 V *vs.* SCE In 3.5 % NaCl	190	[32]
316L SS	0.02 M $ZnCl_2$, 0.1 M $NiSO_4$, 0.4 M H_3BO_4, 1 M Na_2SO_4, 0.335 M triethanolamine	-0.5 V *vs.* Ag/AgCl in 3.5 % NaCl	0.535	Present work

Figure 10 shows representative surface morphologies of selected Zn-Ni alloys: Zn:Ni (1:1) with presence of sucrose, Zn:Ni (1:5) without additives, and Zn:Ni (1:5) with the presence of triethanolamine, respectively. In the case of (Zn:Ni) with sucrose (Figure 10A), it can be seen dendritic growth with a more porosity structure, which refers to a mass transport-controlled electrocrystallization process. In addition, from Figure 10A, it can be seen significant cracks in the deposits, while in the case of Zn:Ni (1:5) without additives (Figure 10B), cracks can be rarely seen in the deposits, which are fairly uniform and coordinated in a pyramidal like form.

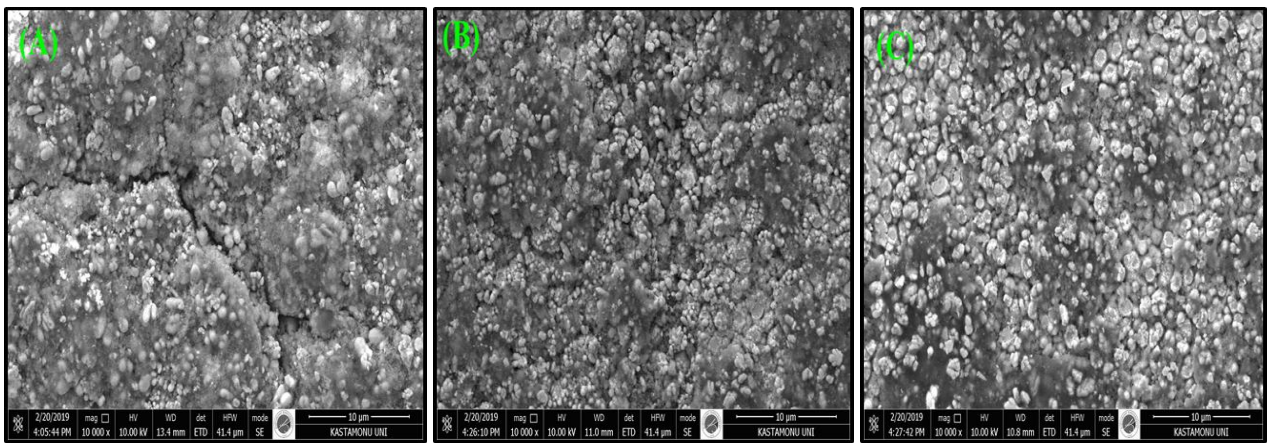

Figure 10. *SEM images of Zn-Ni alloy deposited from: A) 0.02 M $ZnCl_2$ + 0.02 M $NiSO_4$, 0.4 M H_3BO_4, 1 M Na_2SO_4 with 0.015 M sucrose; B) 0.02 M $ZnCl_2$ + 0.1 M $NiSO_4$, C) 0.02 M $ZnCl_2$ + 0.1 M $NiSO_4$, 0.4 M H_3BO_4 1 M Na_2SO_4, with 0.335 M triethanolamine*

From Figure 10C, it can be seen that a more uniform and homogenous growth process with a circular cross-section, less porosity layer without cracks in the deposits produced from a bath

containing Zn:Ni (1:5) with triethanolamine. This granular coating may be related to the higher concentration of nickel with the presence of triethanolamine, leading to improved corrosion resistance of the coating layer [43].

Figure 11 shows representative EDX spectra of selected Zn-Ni alloys: Zn:Ni (1:1) with the presence of sucrose, Zn:Ni (1:5) without additives, and Zn:Ni (1:5) with the presence of triethanolamine respectively. It can be seen from Figure 11A that the composition ratio is 28.14/25.29 (Ni-Zn), while Figure 11B shows a composition ratio of 30.64/17.49 (Ni-Zn), and the last one in Figure 11C shows a composition ratio of 33.04/16.18 (Ni-Zn). The results confirmed the presence of nickel and zinc on the surface, and these properties explain why corrosion resistance is enhanced with the presence of additives.

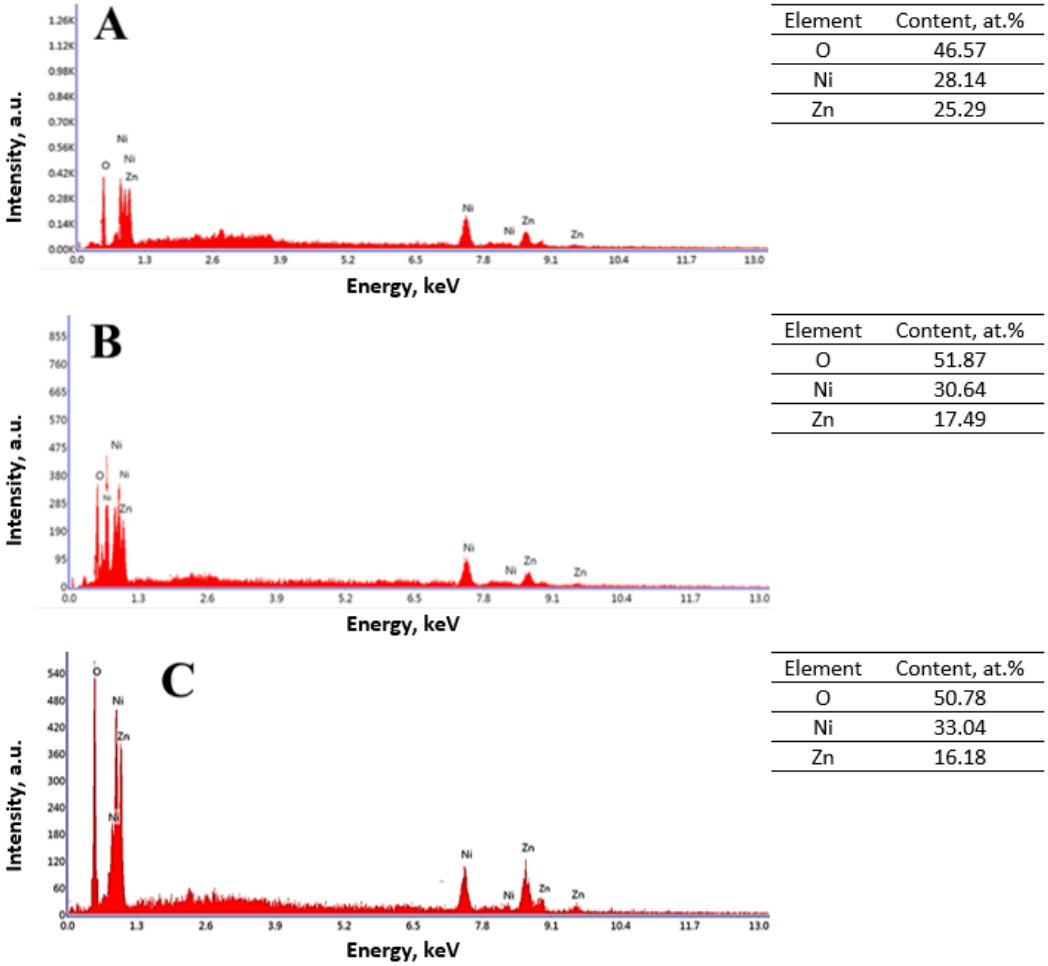

Figure 11. *EDX spectra of Zn-Ni alloys deposited from: A) 0.02 M $ZnCl_2$ + 0.02 M $NiSO_4$, 0.4 M H_3BO_4, 1 M Na_2SO_4 with 0.015 M sucrose; B) 0.02 M $ZnCl_2$ + 0.1 M $NiSO_4$, C) 0.02 M $ZnCl_2$, + 0.1 M $NiSO_4$, 0.4 M H_3BO_4 1 M Na_2SO_4, with 0.335 M triethanolamine*

Conclusions

The corrosion protection of stainless steel in 3.5 % NaCl solution was greatly improved by Zn-Ni coating deposited with additives (triethanolamine or sucrose) at applied constant cathodic potential of -1.3 V. Cyclic voltammetry experiments showed multiple oxidation peaks confirming that different intermediate phases are formed during electrodeposition of Zn-Ni alloy on stainless steel. The corrosion resistance of Zn-Ni alloys increases by increasing nickel concentration and the addition of triethanolamine. Based on the potentiodynamic polarization curves, it can be concluded that Zn-Ni alloys have higher corrosion resistance in synthetic seawater (3.5 % NaCl) than Zn alone.

(cc) BY

This is due to a strong protected layer of zinc-nickel alloys that prevents aggressive ions from attacking the surface. The corrosion rates were remarkably slowed down from 0.022 mm/year without coating (316L SS) to 0.0096 and 0.00795 mm/year with coatings Zn:Ni (1:5) + 0.4 M H_3BO_4 and Zn:Ni (1:5) + 0.4 M H_3BO_4 + 0.335 M triethanolamine, respectively. Triethanolamine additive, possibly by its preferential surface adsorption, showed a more pronounced effect on the deposition compared to the sucrose additive.

Scanning electron microscope images (SEM) revealed a compact deposition of dendrites with cracks on the coating surface deposited from Zn:Ni (1:1) + 0.4 M H_3BO_4 + 0.015 M sucrose. On the other side, the coating deposited from Zn:Ni (1:5) + 0.4 M H_3BO_4 + 0.33 5 M triethanolamine showed strong adhesion, no cracks, more homogeneous growth layer, and less porous structure, which reduced the aggressive ions to ingress to the stainless steel surface. The SEM findings comply with the tests of potentiodynamic polarization according to the reasons mentioned above.

Acknowledgments: *Authors wish to acknowledge the helpful suggestions and gracious technical assistance from the staff of the Chemical Engineering Department, and Materials of Engineering Department, College of Engineering-University of Al-Qadisiyah.*

References

[1] Q. Hu, G. Zhang, Y. Qiu, X. Guo, The crevice corrosion behaviour of stainless steel in sodium chloride solution, *Corrosion Science* **53** (2011) 4065-4072. https://doi.org/10.1016/j.corsci.2011.08.012

[2] F. Azizi, A. Kahoul, Electrodeposition and corrosion behaviour of Zn-Co coating produced from a sulphate bath, *Transactions of the IMF* **94** (2016) 43-48. https://doi.org/10.1080/00202967.2015.1122917

[3] I.H. Karahan, H.S. Güder, Electrodeposition and properties of Zn, Zn-Ni, Zn-Fe and Zn-Fe-Ni alloys from acidic chloride-sulphate electrolytes, *Transactions of the IMF* **87** (2009) 155-158. https://doi.org/10.1179/174591909X438875

[4] R. Fratesi, G. Roventi, Electrodeposition of zinc-nickel alloy coatings from a chloride bath containing NH 4 Cl, *Journal of Applied Electrochemistry* **22** (1992) 657-662. https://doi.org/10.1007/BF01092615

[5] K.O. Nayana, T. V Venkatesha, K.G. Chandrappa, Influence of additive on nanocrystalline, bright Zn-Fe alloy electrodeposition and its properties, *Surface and Coatings Technology* **235** (2013) 461-468. https://doi.org/10.1016/j.surfcoat.2013.08.003

[6] Y. Lin, J.R. Selman, Electrodeposition of corrosion-resistant Ni-Zn alloy: I. Cyclic voltammetric study, *Journal of The Electrochemical Society* **140** (1993) 1299. https://doi.org/10.1149/1.2220974

[7] B. Mojarad Shafiee, R. Torkaman, M. Mahmoudi, R. Emadi, E. karamian, An improvement in corrosion resistance of 316L AISI coated using PCL-gelatin composite by dip-coating method, *Progress in Organic Coatings* **130** (2019) 200-205. https://doi.org/10.1016/j.porgcoat.2019.01.057

[8] R. Fujisawa, M. Sakaihara, Y. Kurata, Y. Watanabe, Corrosion behaviour of nickel base alloys and 316 stainless steel in supercritical water under alkaline conditions. *Corrosion Engineering, Science and Technology* **40(3)** (2005) 244-248. https://doi.org/10.1179/174327805X66308

[9] M. Wang, S. Zeng, H. Zhang, M. Zhu, C. Lei, B. Li, Corrosion behaviors of 316 stainless steel and Inconel 625 alloy in chloride molten salts for solar energy storage, *High Temperature Materials and Processes* **39(1)** (2020) 340-350. https://doi.org/10.1515/htmp-2020-0077

[10] J.R. Davis, *Stainless Steels*, ASM International, 1994. https://books.google.iq/books?id=OrlG98AHdoAC
[11] L. Wei, X. Pang, K. Gao, Effect of flow rate on localized corrosion of X70 steel in supercritical CO_2 environments, *Corrosion Science* **136** (2018) 339-351. https://doi.org/10.1016/j.corsci.2018.03.020
[12] A. Brenner, Electrodeposition of Alloys: Principles and Practice, Elsevier, 2013. ISBN 978-14832231-17
[13] G. Roventi, R. Fratesi, R.A. Della Guardia, G. Barucca, Normal and anomalous codeposition of Zn-Ni alloys from chloride bath, *Journal of Applied Electrochemistry* **30** (2000) 173-179. https://doi.org/10.1023/A:1003820423207
[14] S.H. Mosavat, M.H. Shariat, M.E. Bahrololoom, Study of corrosion performance of electrodeposited nanocrystalline Zn-Ni alloy coatings, *Corrosion Science* **59** (2012) 81-87. https://doi.org/10.1016/j.corsci.2012.02.012
[15] H. Conrad, J. Corbett, T.D. Golden, Electrochemical deposition of γ-phase zinc-nickel alloys from alkaline solution, *ECS Transactions.* **33** (2011) 85. https://doi.org/10.1149/1.3566091
[16] H. M. Abd El-Lateef, E.-S. Abdel-Rahman, H. S. Mohran, Role of Ni content in improvement of corrosion resistance of Zn-Ni alloy in 3.5% NaCl solution. Part I: Polarization and impedance studies, *Transactions of Nonferrous Metals Society of China* **25** (2015) 2807-2816. https://doi.org/10.1016/S1003-6326(15)63906-1
[17] E. Beltowska-Lehman, P. Ozga, Z. Swiatek, C. Lupi, Electrodeposition of Zn-Ni protective coatings from sulfate-acetate baths, *Surface and Coatings Technology* **151** (2002) 444-448. https://doi.org/10.1016/S0257-8972(01)01614-0
[18] D. E. Hall, Electrodeposited Zinc--Nickel Alloy Coatings, *Plating and Surface Finishing* **70** (1983) 59-65.
[19] J. B. Bajat, M. D. Maksimović, V. B. Mišković-Stanković, S. Zec, Electrodeposition and characterization of Zn-Ni alloys as sublayers for epoxy coating deposition, *Journal of Applied Electrochemistry* **31** (2001) 355-361. https://doi.org/10.1023/A:1017580019551
[20] A. Petrauskas, L. Grincevičienė, A. Česūnienė, E. Matulionis, Stripping of Zn-Ni alloys deposited in acetate-chloride electrolyte under potentiodynamic and galvanostatic conditions, *Surface and Coatings Technology* **192** (2005) 299-304. https://doi.org/10.1016/j.surfcoat.2004.08.191
[21] R. G. Baker, C. A. Holden, Zinc-nickel alloy electrodeposits: rack plating, *Plating and Surface Finishing* **72** (1985) 54-57. https://api.semanticscholar.org/CorpusID:100382391
[22] K. Wykpis, M. Popczyk, A. Budniok, Electrolytic deposition and corrosion resistance of Zn-Ni coatings obtained from sulphate-chloride bath, *Bulletin of Materials Science* **34** (2011) 997-1001. https://doi.org/10.1007/s12034-011-0228-8
[23] H. Nakano, S. Arakawa, Y. Takada, S. Oue, S. Kobayashi, Electrodeposition Behavior of a Zn-Ni Alloy in an Alkaline Zincate Solution, *Materials Transactions* **53** (2012) 1946-1951. https://doi.org/10.2320/matertrans.M2012241
[24] L.S. Tsybulskaya, T. V Gaevskaya, O.G. Purovskaya, T. V Byk, Electrochemical deposition of zinc-nickel alloy coatings in a polyligand alkaline bath, *Surface and Coatings Technology* **203** (2008) 234-239. https://doi.org/10.1016/j.surfcoat.2008.08.067
[25] M. G. Hosseini, H. Ashassi-Sorkhabi, H. A. Y. Ghiasvand, Electrochemical studies of Zn-Ni alloy coatings from non-cyanide alkaline bath containing tartrate as complexing agent, *Surface and Coatings Technology* **202** (2008) 2897-2904. https://doi.org/10.1016/j.surfcoat.2007.10.022
[26] M. Li, S. Luo, Y. Qian, W. Zhang, L. Jiang, J. Shen, Effect of additives on electrodeposition of nanocrystalline zinc from acidic sulfate solutions, *Journal of The Electrochemical Society* **154** (2007) D567. https://doi.org/10.1149/1.2772093

(cc) BY

[27] O. Hammami, L. Dhouibi, P. Berçot, E. M. Rezrazi, E. Triki, Effect of diethanolamine and triethanolamine on the properties of electroplated Zn-Ni alloy coatings from acid bath, *Canadian Journal of Chemical Engineering* **91** (2013) 19-26. https://doi.org/10.1002/cjce.21627
[28] V. Ravindran, V. S. Muralidharan, Zinc-Nickel Alloy Electrodeposition-Influence of Triethanolamine, *Portugaliae Electrochimica Acta* **25** (2007) 391. https://doi.org/10.4152/pea.200704391
[29] H. Z. Zardini, M. Davarpanah, M. Shanbedi, A. Amiri, M. Maghrebi, L. Ebrahimi, Microbial toxicity of ethanolamines - Multiwalled carbon nanotubes, *Journal of Biomedical Materials Research A* **102** (2014) 1774-1781. https://doi.org/10.1002/jbm.a.34846
[30] R. J. Ludwig, W. E. Rosenberg, Brightener additive and bath for alkaline cyanide-free zinc electroplating, US20040084322A1 (2004).
[31] C. A. Loto, Electrodeposition of zinc from acid based solutions: a review and experimental study, *Asian Journal of Applied Sciences* **5(6)** (2012) 314-326. 10.3923/ajaps.2012.314.326
[32] H. Faid, L. Mentar, M. R. Khelladi, A. Azizi, Deposition potential effect on surface properties of Zn-Ni coatings, *Surface Engineering* **33** (2017) 529-535. https://doi.org/10.1080/02670844.2017.1287836
[33] E. Gomez, X. Alcobe, E. Vallés, Characterisation of zinc+ cobalt alloy phases obtained by electrodeposition, *Journal of Electroanalytical Chemistry* **505** (2001) 54-61. https://doi.org/10.1016/S0022-0728(01)00450-8
[34] G. Trejo, R. Ortega, Y. Meas, E. Chaînet, P. Ozil, Effect of benzylideneacetone on the electrodeposition mechanism of Zn-Co alloy, *Journal of Applied Electrochemistry* **33** (2003) 373-379. https://doi.org/10.1023/A:1024466604939
[35] M. Ilayaraja, S. Mohan, R. M. Gnanamuthu, G. Saravanan, Nanocrystalline zinc-nickel alloy deposition using pulse electrodeposition (PED) technique, *Transactions of the IMF* **87** (2009) 145-148. https://doi.org/10.1179/174591909X438947
[36] S. Al Saadi, Y. Yi, P. Cho, C. Jang, P. Beeley, Passivity breakdown of 316L stainless steel during potentiodynamic polarization in NaCl solution, *Corrosion Science* **111** (2016) 720-727. https://doi.org/10.1016/j.corsci.2016.06.011
[37] R. Ramanauskas, P. Quintana, L. Maldonado, R. Pomés, M. A. Pech-Canul, Corrosion resistance and microstructure of electrodeposited Zn and Zn alloy coatings, *Surface and Coatings Technology* **92** (1997) 16-21. https://doi.org/10.1016/S0257-8972(96)03125-8
[38] R. Kumar, S. Obrai, A. Kaur, M. S. Hundal, H. Meehnian, A. K. Jana, Synthesis, crystal structure investigation, DFT analyses and antimicrobial studies of silver (I) complexes with N, N, N', N''-tetrakis (2-hydroxyethyl/propyl) ethylenediamine and tris (2-hydroxyethyl) amine, *New Journal of Chemistry* **38** (2014) 1186-1198. https://doi.org/10.1039/C3NJ00729D
[39] R. P. Sharma, A. Saini, P. Venugopalan, V. Ferretti, F. Spizzo, C. Angeli, C. J. Calzado, Magnetic behaviour vs. structural changes in an isomeric series of binuclear copper (II) complexes: an experimental and theoretical study, *New Journal of Chemistry* **38** (2014) 574-583. https://doi.org/10.1039/C3NJ01080E
[40] H. Zhang, H. Liu, F. Chen, Y. Luo, X. Xiao, Y. Deng, N. Lu, Y. Liu, Microscopic characteristics and corrosion rate modeling in galvanized high-strength steel wires, *Journal of Materials Research and Technology* **33** (2024) 6234-6250. https://doi.org/10.1016/j.jmrt.2024.11.023
[41] M. Ghazi, K. Alfalah, M. Izzettin, Corrosion inhibition potential of new oxo-pyrimidine derivative on mild steel in acidic solution: Experimental and theoretical approaches, *Journal of Molecular Structure* **1315** (2024) 138773. https://doi.org/10.1016/j.molstruc.2024.138773
[42] M. Ghazi Kadhim AlFalah, M. Saracoglu, M. I. Yilmazer, F. Kandemirli, Corrosion inhibition performance of 2- Fluorophenyl-2, 5-dithiohydrazodicarbonamide for copper in 3.5%NaCl

Media: Experimental and Monte Carlo insights, *Al-Qadisiyah Journal for Engineering Sciences* **16** (2023) 150-159. https://doi.org/10.30772/qjes.2023.178995

[43] N. Eliaz, K. Venkatakrishna, A. C. Hegde, Electroplating and characterization of Zn-Ni, Zn-Co and Zn-Ni-Co alloys*, Surface and Coatings Technology* **205** (2010) 1969-1978. https://doi.org/10.1016/j.surfcoat.2010.08.077

©2025 by the authors; licensee IAPC, Zagreb, Croatia. This article is an open-access article distributed under the terms and conditions of the Creative Commons Attribution license (https://creativecommons.org/licenses/by/4.0/)